Microfluidic Digital PCR for Multigene Analysis of Individual Environmental Bacteria

Abstract

Gene inventory and metagenomic techniques have allowed rapid exploration of bacterial diversity and the potential physiologies present within microbial communities. However, it remains nontrivial to discover the identities of environmental bacteria carrying two or more genes of interest. We have employed microfluidic digital PCR to amplify and analyze multiple, different genes obtained from single bacterial cells harvested from nature. A gene encoding a key enzyme involved in the mutualistic symbiosis occurring between termites and their gut microbiota was used as an experimental hook to discover the previously unknown rRNA-based species identity of several symbionts. The ability to systematically identify bacteria carrying a particular gene and to link any two or more genes of interest to single species residing in complex ecosystems opens up new opportunities for research on the environment.

Article Text

A major challenge of environmental science is the identification of microbial species capable of catalyzing important activities *in situ* (12). PCR-based techniques that use single genes as proxies for organisms or key microbial activities continue to provide valuable insights into microbial community diversity (17, 44, 60). However, it has been difficult to interrelate PCR-derived gene inventories to derive correspondences between any two or more specific genes of interest, or to determine the phylogenetic species identity of organisms carrying particular genetic capabilities. Metagenomic (41) analyses of complex communities are dominated by genome "shrapnel"; unless the microbial community is dominated by one or a few species (45, 50) resident genomes are not reliably reconstructed via computation (49, 51). A gene of interest can be attributed to a specific organism only if it is linked to an unambiguous phylogenetic marker, i.e., on the same genome fragment (7, 41). Both PCR and metagenomic studies are typically carried out on homogenized, whole-community genomic DNA preparations. Thus the cell as a distinct informational entity is almost entirely lost.

Outside of traditional culture-based isolation, few approaches can attribute multiple genes to a single species or cell type. Microautoradiography (33) and stable isotope probing (31) allow detection of cells or retrieval of genetic material from organisms utilizing a substrate of interest, but require active cellular incorporation of that substrate. Microscopy-based *in situ* hybridization-based techniques (FISH and variants (5, 61)) allow colocalization of sequences through probe hybridization, but require that both genes be 1) actively transcribed and their sequences 2) be known in advance and 3) be of

sufficient difference from related, nontarget genes for effective probe design and implementation. Single cell whole genome amplification has recently been reported for a highly abundant, culturable marine microbial species, but has not yet been shown to be scalable to interrogating multitudes of diverse, coresident microbes (59). Here, we have applied microfluidic devices to perform a variant of "digital PCR" (52), separating and interrogating hundreds of individual environmental bacteria in parallel.

Microfluidic devices allow control and manipulation of small volumes of liquid (14, 48), in this case allowing for rapid separation and partitioning of single cells from a complex parent sample. Single, partitioned cells served as templates for individual multiplex PCR reactions using primers and probes for simultaneous amplification of both small-subunit ribosomal RNA and metabolic genes of interest. Primers and probes with broad target specificities were employed with subsequent resolution of exact gene sequences after successful amplification and retrieval. This technique operates independent of gene expression, position of the gene on the genome, and the physiological state of the cell at the time of harvest. This resulted in the rapid colocalization of two genes (encoding 16S rRNA and a key metabolic enzyme) to single genome templates, along with the determination of the fraction of cells within the community that encoded them. Subsequent retrieval of PCR products from individual chambers allowed sequence analysis of both genes; phylogenetic analysis of the ribosomal RNA gene allows classification of the host bacterium and the metabolic gene is sequenced to confirm the cell carried the genotype of interest. Additionally, since microfluidic digital PCR yields fluorescent signal upon amplification of a gene regardless of the number of copies

present the cell, this approach can yield estimates of the fraction given species represent within the general microbial community. The number of *rrn* operons present in a genome can vary widely, ranging from 1 (e.g., *Rickettsia prowazekii* (37)) to 15 (e.g., *C. paradoxum* (40)), confounding the interpretation of traditional environmental gene inventories. Moreover, the use of single cell PCR to prepare clone libraries will avoid complications and PCR artifacts such as amplification biases and unresolvable chimeric products (4).

We employed this technique to examine a complex, species-rich environment: the lignocellulose-decomposing microbial community resident in the hindguts of wood-feeding termites. Therein, the bacterial metabolism known as CO_2-reductive homoacetogenesis is one of the major sources of the bacterial fermentation product, acetate (10). Acetogenic bacteria must compete for hydrogen with *Archaea* that generate methane, a potent greenhouse gas for which termites are considered a small yet significant source. Because of their high rates of bacterially mediated homoacetogenesis, many termites contribute significantly much less to the global methane budget than they might otherwise (8). Additionally, acetate serves as the insect host's major carbon and energy source, literally fueling a large proportion of this mutualistic symbiosis (10, 35, 47). A key gene of the homoacetogenesis pathway encodes formyl-tetrahydrofolate synthetase (FTHFS) (27). Previously, a diversity of termite hindgut community FTHFS variants were inventoried (42), but the identities of the organisms dominating homoacetogenesis in termites had remained uncertain. Here using microfluidics, we

discovered the identities of a multitude of FTHFS-encoding organisms by determining their specific 16S rRNA gene sequences.

The *"Clone H Group"* of FTHFS genotypes corresponds to a large fraction of the sequences collected during an inventory of FTHFS genes present in the termite hindgut environment (42). We designed a specific primer set and a fluorescein-labeled probe capable of on-chip detection and amplification of the genotypes comprising this FTHFS group. We also redesigned broad-specificity "*all bacterial*" 16S rRNA gene primers and employed a previously published probe (46) to amplify and detect bacterial rRNA genes. Both the all bacterial 16S rRNA gene and Clone H Group FTHFS primer/probe sets showed single molecule sensitivity in multiplex on-chip reactions using purified plasmid or termite gut community DNA. The observed success rate for the amplification of individual genes from single molecule templates was 40% (see chapter appendix), thus the success rate for coamplification of two genes from single molecule templates is estimated to be ca. 1 in 7.

Freshly collected termite hindgut contents were suspended in a PCR reaction buffer and loaded into a microfluidic device. Each microfluidic panel uses micromechanical valves to randomly partition a single PCR mixture into 1,176 independent 6.25 nL reaction chambers (Figure 4.1). We considered single-cell separation to be achieved when fewer than one third of chambers showed rRNA gene amplification. Assuming a Poisson distribution of cells, under such conditions 6% of chambers should have contained multiple cells or cell aggregates (1). PCR was carried out on a conventional flat-block

4-6

thermocycler. Amplification was monitored using 5´ nuclease probes to generate a

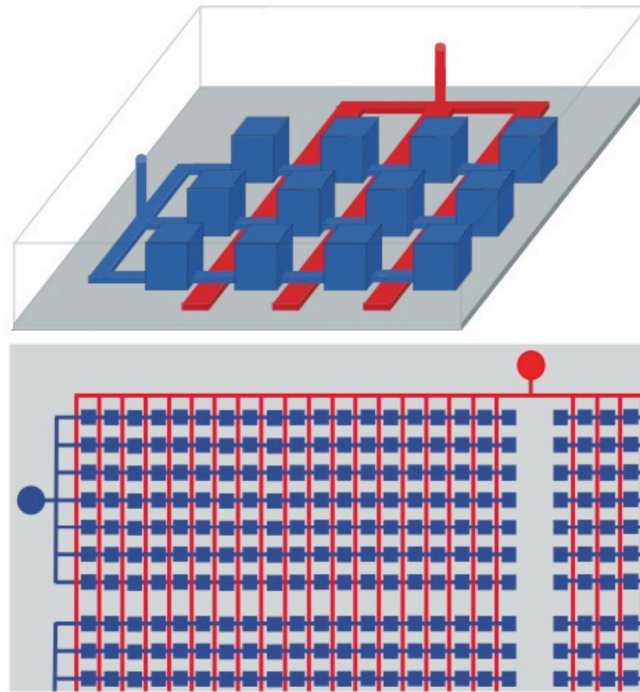fluorescent signal detected with a modified microarray scanner.

Figure 4.1. Microfluidic Digital PCR Chip Architecture. **Top**, schematic diagram
showing many parallel chambers (blue) connected by channels to a single input. When
pressure is applied to the control channel network (red), the membranes between the red
and blue channels are deflected upward, creating micromechanical valves. When the
valves are closed, the continuous blue network is partitioned into independent PCR
reactors. **Bottom**, schematic showing how a single valve connection can be used to
partition thousands of chambers. In the device used, each experimental sample could be
partitioned into 1,176 chambers, and each device contained 12 such sample panels.

Multiplex PCR amplifications from single cells or cell aggregates were successfully

performed using diluted gut contents that had been partitioned on-chip (Figure 4.2, left).

We found global averages of 1.2 ± 0.8 x 10^8 total bacterial 16S rRNA gene encoding

units and 1.5 ± 1.0 x 10^6 total Clone H Group FTHFS gene encoding units per

Zootermopsis nevadensis termite (2) This suggests that, in *Z. nevadensis*, these particular

FTHFS genes are carried by a minority population representing ca. 1% of gut symbionts.

The observed variability of these measurements was not surprising as the *Z. nevadensis*

specimens examined were collected from different colonies and locations, and had been
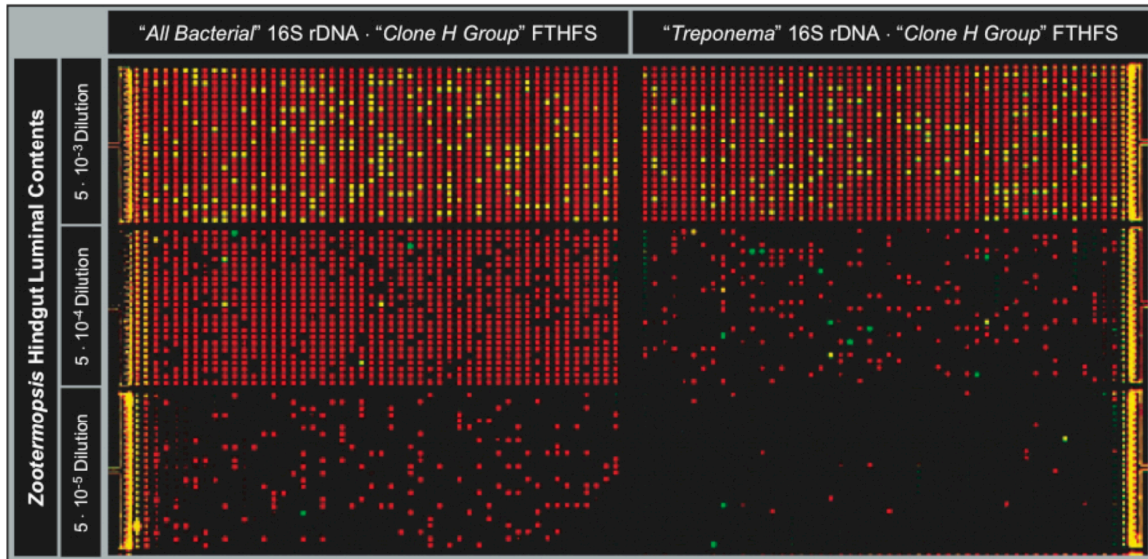
maintained in captivity for varying periods of time.

Figure 4.2. Multiplex microfluidic digital PCR of single cells in environmental samples. Six panels from a representative experiment showing microfluidic digital PCR on hindgut contents harvested from a single *Z. nevadensis* individual. Left, multiplex PCR using "all bacterial" 16S rRNA gene (red fluorescence) and "Clone H Group" (42) FTHFS gene (green fluorescence) primers and probes. Reaction chambers that contained both genes in 1/500,000 dilutions from this and other on-chip experiments were sampled and the PCR products were analyzed (see Figure 4.5). Right, the same, except that 16S rRNA primers specifically targeted members of the "termite cluster" (26) of the spirochetal genus *Treponema*.

Amplification products were retrieved from reaction chambers via syringe needle and

were reamplified, cloned, sequenced, and analysed using standard methods. Twenty

randomly selected chambers that had amplified only a 16S rRNA gene (and not FTHFS)

yielded a diversity of *Endomicrobia*, *Firmicutes*, *Bacteroidetes*, *Proteobacteria* and

Spirocheates ribotypes that was expected based upon prior 16S rRNA gene clone

libraries (36) (Figure 4.3 & 4.4). Two thirds of chambers positive for FTHFS genes did

not amplify 16S rRNA genes when either all bacterial or termite treponeme-specific

rRNA gene primers were employed. This amplification success rate is comparable to that

observed when purified, single molecule templates were used and remains a target of
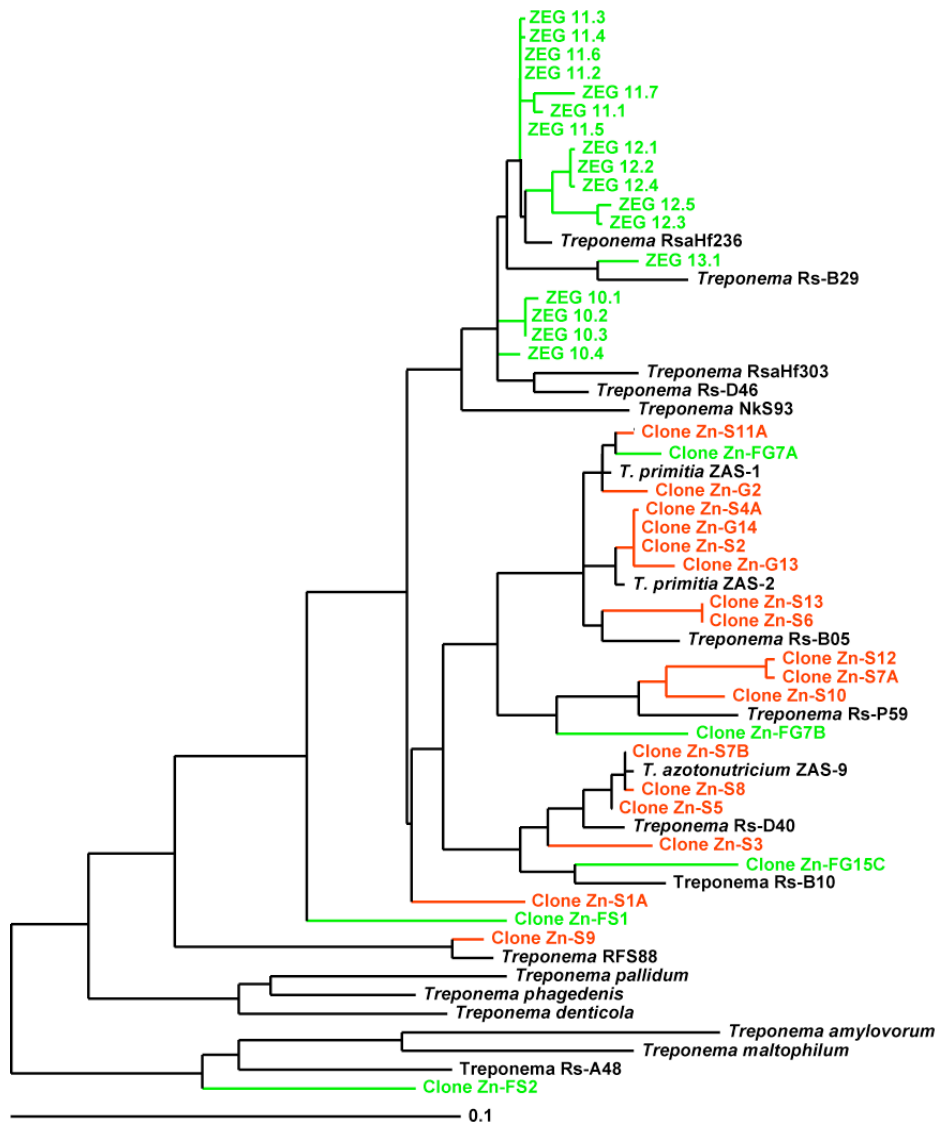
refinement and improvement in the future.

Figure 4.3. Phylogenetic Analysis of *Treponemal* 16S rRNA sequences retrieved from microfluidic chips. Sequences recovered from chambers in which only 16S rRNA genes were amplified are marked in red; a Zn-G moniker denotes that "*all bacterial*" primers were employed, Zn-S spirochete-specific primers. Sequences corecovered with FTHFS sequences are marked in green; those that fell outside the ZEG cluster were assigned a Zn-FG or Zn-FS moniker according to the 16S rRNA primer set employed. ZEG 11.5-11.7 and 12.5 were identified in experiments using spirochete-specific rRNA primers. Tree calculated using Phylip distance methods and 630 unambiguous, aligned residues. Scale bar represents 0.1 changes per alignment position.
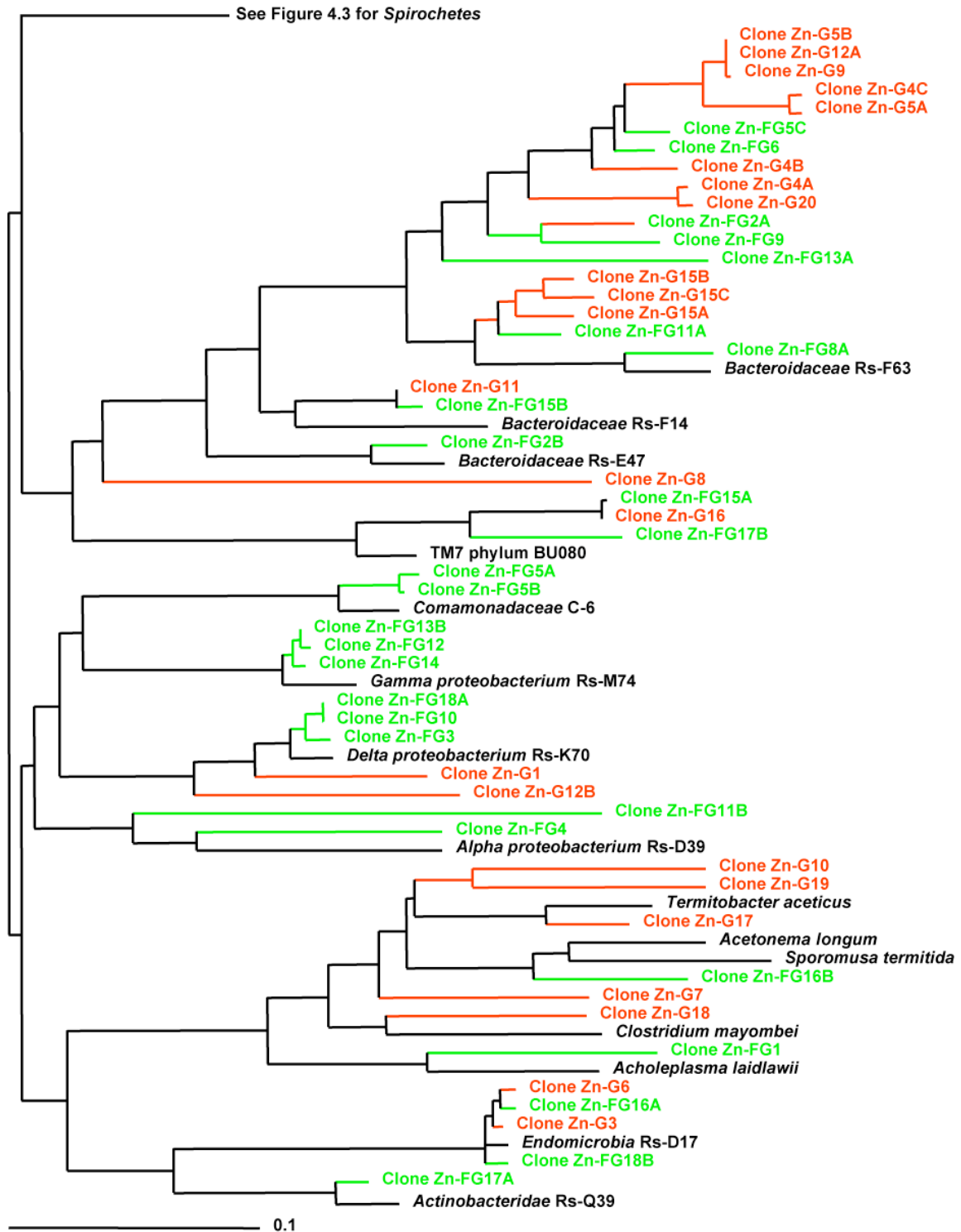
Figure 4.4. Phylogenetic Analysis of 16S rRNA sequences retrieved from microfluidic chips and close relatives. Sequence naming and color coding as described in Figure 4.3. Tree was calculated using Phylip distance methods and 630 unambiguous, unaligned residues. Scale bar represents 0.1 changes per alignment position.

PCR products were retrieved and analyzed from 28 reaction chambers that coamplified both FTHFS and 16S rRNA genes. In ten of those reactions, sequence analyses revealed that the FTHFS gene had coamplified with a clade of closely related 16S rRNA gene sequences affiliating with within the "termite spirochete cluster" (26) of the genus *Treponema*. Members of this novel clade were never observed in chambers that lacked FTHFS gene amplification. An additional three chambers contained a single FTHFS type and multiple 16S rRNA genotypes, one of which in each affiliated with the above mentioned group (ZEG 11.4, 10.2, 10.1). These latter reactions also contained: two additional other *Spirochaetes* (Zn-FG7A&B in Figure 4.3) in one chamber, a single γ-*Proteobacterium* sequence (Zn-FG12) in the second, and a *Firmicutes* sequence (ZN-FG1) in the third. The remaining fifteen chambers analyzed (that coamplified FTHFS and rRNA genes) yielded 16S rDNA sequences in proportions that corresponded well with the ribotype diversity encountered in the general non-FTHFS encoding population. Based on this evidence, we conclude that the unique cluster of termite gut treponeme rRNA gene sequences that were repeatedly identified in FTHFS-containing chambers represent the ribotype of the FTHFS-encoding cells. We attribute the instances of FTHFS colocalization with other rRNA gene sequences to cell-cell aggregations. The latter is not to be unexpected in a complex, wood-particle-filled and sticky environment such as the termite hindgut (9, 21). Such aggregations appear to be largely random, though there may be a slight enrichment of proteobacterial sequences in comparison to the general population (Figure 4.4). Our results show that FTHFS sequences present in ca. 1% of all bacterial cells were, in 13 out of 28 trials, found in association with a 16S rRNA sequence type not identified in 20 random samplings of the all bacterial population

(16S rRNA only chambers) at large. The probability of a 16S rRNA gene sequence type that is present at less than 5% of the population randomly colocalizing with FTHFS in 13 out of 28 trials is low, on the order of 10^{-10} (3).
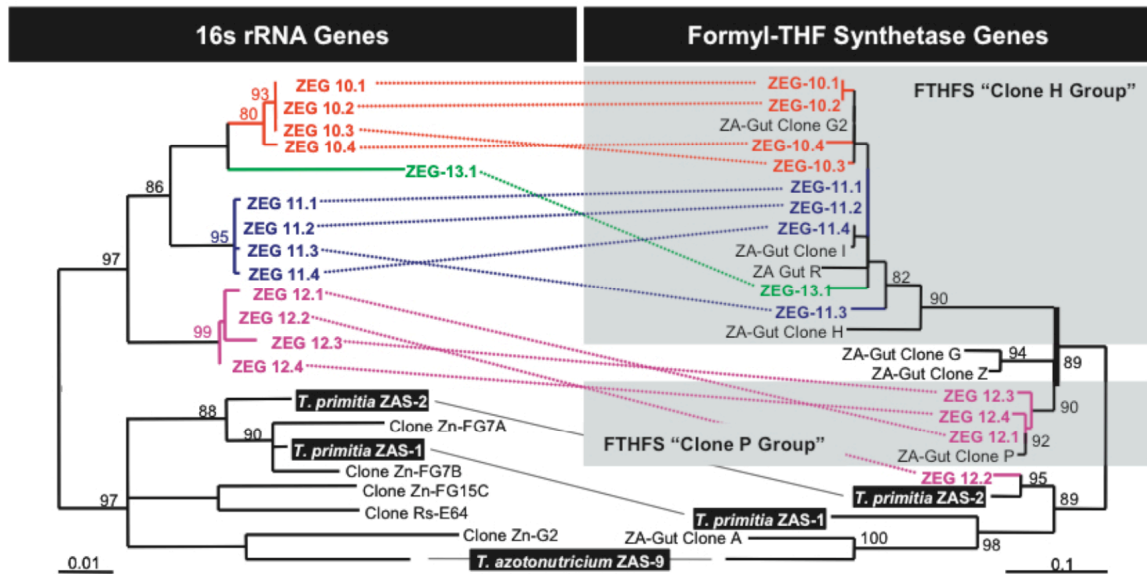

Figure 4.5. "*Clone H*" and "*Clone P Group*" FTHFS genes are encoded by not-yet-cultivated termite gut treponemes. **Left**, phylogenetic tree of 16S rRNA genes cloned from cultivated strain isolates (orange) and from hindgut community microbiota. **Right**, phylogenetic tree of FTHFS genes from the termite hindgut. Dotted lines connect genes believed to originate from the same genome. Incongruent gene phylogenies implicate acquisition of FTHFS genes via lateral gene-transfer and can be observed in both isolated species (*T. primitia* ZAS-1) and proposed "environmental genomovars" (ZEG 12.2). Scale bars represent substitutions per alignment position. The trees were constructed using TreePuzzle (43); 630 (16S rDNA) and 249 (FTHFS) nucleotide positions were used.

Refined phylogenetic analysis of 16S rRNA gene sequences that were repeatedly isolated from FTHFS-containing reaction chambers revealed that all such 16S rRNA gene sequences affiliated within the termite gut treponeme cluster of *Spirochaetes*. These 16S rRNA genes group into four distinct ribotype clusters (Figure 4.5). These four sequence types share >99% sequence identity within-group and between-group identities of 95%–99%. We propose the term "*environmental genomovar*" (genome variant) to describe

not-yet-cultivated organisms shown to encode two or more known genes of interest. Here, we use the epithets ZEG-10 (for $\underline{Z}$ootermopsis $\underline{E}$nvironmental $\underline{G}$enomovar) through ZEG-13 to describe the four 16S ribotypes identified (9 termite gut treponemes have been isolated and assigned the strain epithets ZAS-1 (for $\underline{Z}$ootermopsis $\underline{A}$cetogenic $\underline{S}$pirochete) through ZAS-9 (22, 25)). Genomovars ZEG-10, 11, and 13 encode Clone H Group FTHFS sequences, while one ZEG-12 genomovar encodes a Clone P Group FTHFS sequence.

To build additional support for a spirochetal origin of Clone H Group FTHFS genotypes, we designed and employed a termite treponeme-specific 16S rRNA gene primer set and gene probe, with the aim of reducing nonspirochetal background (Figure 4.2, right). The frequency with which Clone H Group FTHFS genes were recovered increased from 1 in 175 cells of the general bacterial population, to 1 in 16 treponemal cells (several termite gut treponemes are already known or suspected to encode FTHFS genotypic variants that would not amplify with the Clone H group FTHFS primer and probe set (42), see Figure 4.3). Similar to the amplification success rates observed in experiments using the "all bacterial" 16S rRNA gene primers (Figure 4.2, left) and those using the Clone H primers against purified single molecule templates ca. 1/3 of FTHFS-positive reaction chambers also amplified detectable levels of 16S rRNA gene. Treponemal cells were deduced to comprise 10%–12% of the bacterial community of *Z. nevadensis* (comparing amplification frequencies in the left and right panels of Figure 4.2). These results are in good agreement with the results of a traditional 16S rRNA clone inventory from *Z.*

nevadensis, which suggested that 15% of clones corresponded to treponemes (unpublished data).

In summary: specific not-yet-cultivated *Treponema* species encode variants of a key gene underlying the dominant bacterial metabolism known to impact the energy needs of their termite hosts. The microfluidic, multiplex digital PCR approach taken here can be extended to expand our understanding of the genetic capacities of not-yet-cultivated species, and to collect and collate genetic information in a manner that builds conceptual genomovars that directly represent the organisms catalyzing important activities in various environments of global relevance.

Materials and Methods

Termite Maintenance

Zootermopsis nevadensis specimens were collected from fallen Jeffrey (*Pinus jeffreyi*) and Ponderosa Pine (*Pinus ponderosa*) at Mt. Pinos in the Los Padres National Forest and at the Chilao Campground in the Angeles National Forest. Colonies were maintained in the laboratory on Ponderosa at 23 °C and at a constant humidity of 96%, achieved via incubation over saturated solutions of KH_2PO_4 within 10-gallon aquaria (55).

PCR on Microfluidic Chips

Microfluidic devices were purchased from Fluidigm Corporation (www.fluidigm.com/didIFC.htm). On-chip multiplex PCR reactions contained 0.05 units μL^{-1} iTaq DNA polymerase (BioRad), iTaq PCR buffer, 200 μM each dNTP, 1.5 mM

MgCl$_2$, and 0.1% Tween-20. In almost all PCR reactions, primers and probes were used at 400 nM; all bacterial 16S primers were used at 600 nM in on-chip reactions. Primers and probes were purchased from Integrated DNA Tecnologies and had the following sequences: FTHFS forward, 5′-GAATCACGCGAAGACTGGTTC-3′; reverse, 5′-TTGAGTTACAACCGTGTGCGAT-3′; probe, 5′-CAAGGCGCAATGGCAGCCCT-3′ (FAM and Black Hole Quencher 1 labelled), all bacterial rRNA 357 forward 5′-CTCCTACGGGAGGCAGCAG-3′ (modified from (32)), 1492 reverse 5′-TACGGYTACCTTGTTACGACTT-3′ (modified from (20)); 1389 reverse probe 5′-CTTGTACACACCGCCCGTC-3′ (described in (46), labelled with CY5 and Iowa Black quencher). Termite gut spirochete-specific SSU rRNA amplification was achieved using the 1389R probe and 357F primer with a spirochete-specific 1409R primer (sequence 5′-GGGTACCTCCAACTCGGATGGTG-3′).

Zootermopsis hindguts were extracted from worker larvae, suspended in sterile TE (10 mM Tris-HCl, 1 mM EDTA, pH 8), and disrupted via repeated aspiration using a 1 mL Eppendorf pipettor. Suspensions were allowed to stand briefly to sediment large particles, then diluted to working concentrations in TE and mixed 1 to 10 with the PCR reaction mixture (above) for immediate loading onto microfluidic chips.

Chips were loaded using air pressure. 200 µL gel-loading tips were filled with sample and connected to air lines at 12-15 PSI (pounds per square inch) pressure. Control channels were loaded with 35% PEG (polyethylene glycol) 3350 (ca. 50 µL, in gross excess). The 12 sample channels were loaded with 15 µL of PCR reaction (again, in

excess). After loading, sample lines were allowed to reequilibrate to atmospheric pressure. Control valves were closed by the application of 25 PSI air pressure to control lines.

Cycling was carried out on flat-block thermocyclers (MJ Research). Microscope immersion oil (Cargille, Type FF) was applied between the chip and thermocycling block, and the cycling program was as follows: 98 ºC 30 s, 97 ºC 30 s, 95 ºC 2 min, [56 ºC 30 s, 58 ºC 30 s, 60 ºC 30 s, 98 ºC 15 s] x 40 cycles, 60 ºC for 10 min.

Reaction results were evaluated by fluorescent signal strength as measured using an ArrayWoRx scanner (Applied Precision). Spot intensities were located and retrieved using either ArrayWoRx software or the ScanAlyze program (version 2.50, Michael Eisen). Cutoff values for positive amplification were calculated for each sample panel independently. Chambers in the bottom 25% of the intensity range were assumed to contain no amplification, and positive chambers were defined as chambers whose spot intensity was more than 10 standard deviations above the mean of points in this range for the FTHFS probe. The 16S rRNA gene probe gave a more variable signal, so the threshold for this channel was set at 5 standard deviations above the mean.

Sample Retrieval and Analysis

Single-cell PCR products were retrieved from amplification-positive chambers. Chips were peeled from the backing slide, and pressure was removed from control channels (most valves remained fused despite relief of external pressure). Target chambers were

located using a dissecting microscope, and the tip of a 30 gauge syringe needle was inserted into each chamber through the bottom surface of the chip. Needles were then swirled briefly in 10 μL of TE to desorb the PCR product.

Retrieval efficiency was checked by real time PCR using the same primers as above in BioRad SYBR Green PCR Master Mix. Reactions were carried out using the Chromo4 system (BioRad), and temperature program 95 ºC 3 min, (95 ºC 15 s, 60 ºC 1 min30 s) x 40 cycles. FTHFS concentration standards contained a 1.2 kb section of "ZA-gut Clone U" type FTHFS gene sequence (42). Termite community DNA was used as a standard for all bacterial 16S rRNA gene PCR, and *T. primitia* ZAS-2 genomic DNA for spirochete-specific reactions. Samples that contained 104 or more gene copies were deemed successful retrievals.

Retrieved PCR products were amplified for cloning and/or sequencing using EXPAND high fidelity polymerase (Roche), Fail-Safe PCR PreMix D (Epicentre), and primers and cycling conditions as above. PCR products were purified using the Qiagen PCR purification kit, and sequenced using the FTHFS PCR primers and 16S rRNA gene internal primers 1100R and 533F (5′-AGGGTTGCGCTCGTTG-3′ and 5′-GTGCCAGCMGCCGCGGTAA-3′, respectively; modified from ref. (20)). Some samples contained a mixture of 16S rRNA sequences. These sequences were cloned using the TOPO TA cloning kit for sequencing (Invitrogen). Eight colonies from each cloning reaction were picked and used as template for high-fidelity PCR as described above. Ten μL of each reaction was digested at 37 ºC for 2 hr with 3 units HinPI1 from

New England Biolabs and analyzed by agarose gel electrophoresis. A representative of each RFLP (restriction fragment length polymorphism) type was prepared for sequencing as described above, using recommended T3 and T7 primers. All sequencing reactions were carried out by the California Institute of Technology DNA Sequencing Facility.

Sequences were assembled and edited using the Lasergene software package (DNASTAR). Phylogenetic analysis and alignment of 16S rRNA gene sequences was carried out using the ARB software package (30). FTHFS sequences were translated into protein, and aligned using GenomatixSuite software (Genomatix). Nucleic acid sequences were aligned according to the protein alignment. All 16S rRNA gene sequences were screened using chimera identification programs Bellerophon (16) and Pintail (6). Three chimeric sequences were identified and eliminated from further analysis.

Real-Time PCR Standards and DNA Template Preparation

Plasmid templates were purified from *E. coli* strains from the library of Salmassi and Leadbetter using the Qiaprep Spin Miniprep Kit (Qiagen). Termite gut community DNA was extracted from the pooled gut contents of five termites. Guts were disrupted using the protocol laid out in Salmassi and Leadbetter (42), with the substitution of TE (10 mM Tris-HCl, 1 mM EDTA, pH 8) for the phosphate buffer described in that paper. After bead-beating and phenol extraction, DNA was purified from the aqueous phase using the Qiagen DNeasy Tissue kit, with the protocol described for extraction of DNA from crude lysates (DNeasy Tissue Handbook, July 2003 version). Template concentrations were

measured using the Hoefer DyNAQuant 200 fluorometer and DNA quantification system (amersham pharmacia biotech) using reagents and procedures directed in the manual (DQ200-IM, Rev C1, 5-98). Termite gut cell suspensions were prepared as described in the main body of the paper.

Chapter Four Appendix

1. Design and Validation of Primers and Probes for Microfluidic Digital PCR

2. Table 4.1. Sequences used in phylogenetic analysis

Design and Validation of Primers and Probes for Microfluidic Digital PCR

Amplification of Formyl-tetrahydrofolate Synthetase Genes from Termite Gut Acetogens

Primers and probes were designed to specifically amplify FTHFS genes from "*Clone H Group*" acetogens, which comprised 43% of the *Zootermopsis* FTHFS clones inventoried by Salmassi and Leadbetter (42). These primers are distinct from those previously employed to amplify FTHFS genes from pure cultures and environmental samples (23, 24, 28, 39). The newly designed primers and probes were tested for on-chip amplification and specificity using purified plasmid DNA (Figure 4.6). The copy number as deduced from the number of positive chambers detected (adjusted based on a Poisson distribution of template) fell within 11%–110% of the copy number calculated based on the concentration of double-stranded DNA in the template plasmid preparation. Freeze-thaw and template age may be one variable influencing observed amplification efficiencies; it has been recently reported that amplification efficiency can approach 99% (53). A small amount of amplification was detected from closely related clones (Figure 4.6**i**), with a signal to background ratio less than half of that detected in positive clones. This low level of amplification from closely related species was also apparent in later experiments, as several FTHFS clones mapping to the "*Clone P Group*" were retrieved from on-chip reactions (see main text). No fluorescent signal was detected from amplification of distant relatives (clostridial and nonacetogenic FTHFS types, Figure 4.6**k**). FTHFS copies were also detectable within DNA extracted from whole termite guts and from termite gut cell suspensions.

FTHFS simplex experiments used DyNAzyme II polymerase (Finnzymes) at 0.2 units per µl and 1x TaqMan Universal PCR Master Mix (Applied Biosystems) for real-time PCR. Due to the high concentration of detergent in the enzyme storage buffer, only 0.05% Tween-20 (Sigma) was added. All other experiments described used the iTaq system described in the main body of the paper, as this enzyme was found to perform well on the chip at lower concentrations, and had hot-start capabilities to ensure that the enzyme was inactive during the chip loading process.

Design of "All-bacterial" 16S rRNA Primers and Probes

Primers and probes for amplification of bacterial 16S rRNA were also employed. Bacterial 16S rRNA genes detected in on-chip amplification from termite gut community DNA preparation amounted to 1.4×10^5 copies per ng (1 copy every 6.7 MB DNA), which was 5.9-fold higher than the copy number deduced by real-time PCR using *Treponema primitia* ZAS-2 genomic DNA as a standard. Background amplification has been reported in a number of general bacterial 16S real-time assays, and is commonly attributed to DNA fragments present in commercial enzyme preparations (11). In on-chip experiments with the final primer set, negative controls never exceeded 1.2% positive chambers (1.9 copies per µl).
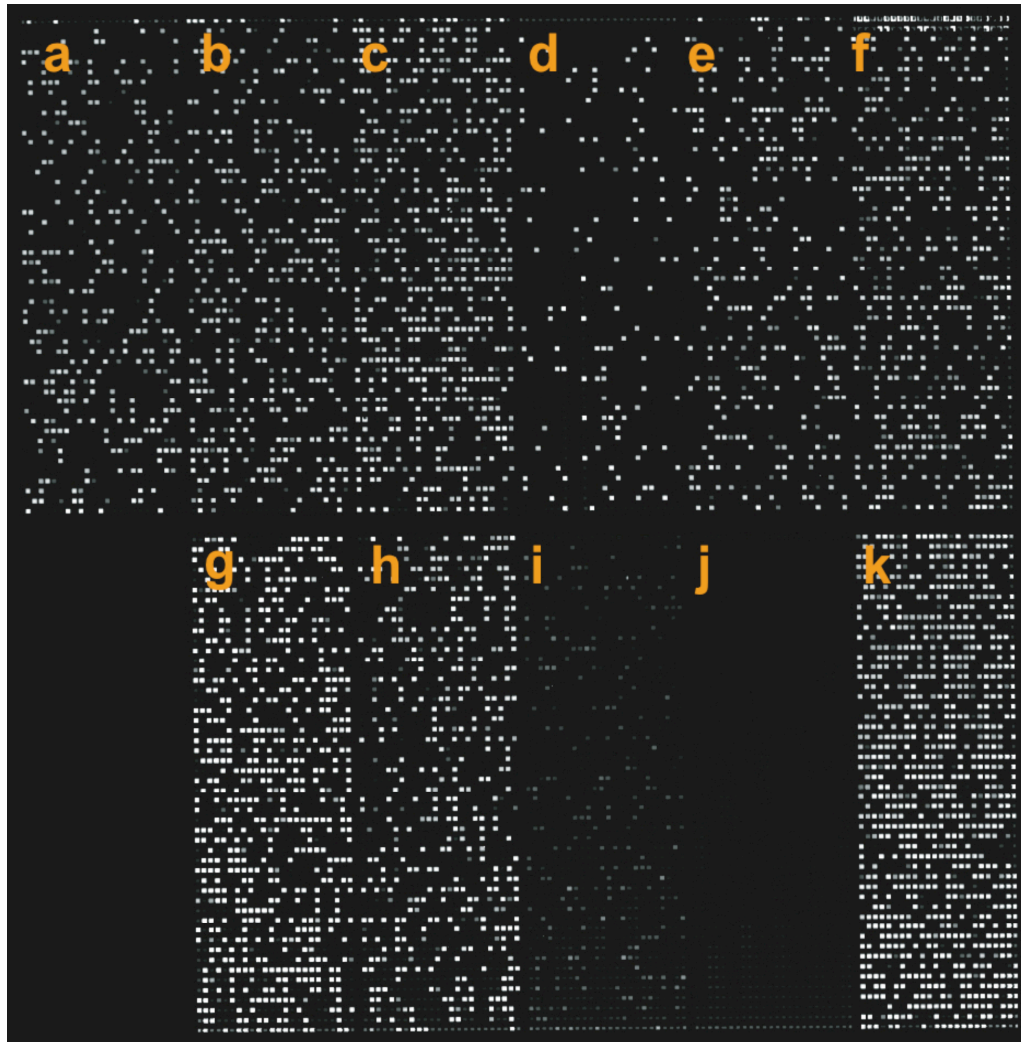
Figure 4.6. FTHFS primer specificity and demonstration of single copy sensitivity. A single microfluidic chip on which the FTHFS primers and probe were tested against purified plasmid templates. Panels a though h and k each show amplification from one of nine different Clone H Group FTHFS genotypes. Panel i contains six pooled non-H type FTHFS genotypes that cluster within the termite Treponeme FTHFS cluster. Panel j contains four pooled FTHFS genotypes that that do not cluster phylogenetically with termite treponemes. All clones (and each clone within pooled templates) were added at DNA concentrations equivalent to ~200 copies per μl. Specific clone types and observed copy number are as follows: a Clone E2, 57 cp/μl; b Clone F2, 70 cp/μl; c Clone G2, 97 cp μl; d Clone H, 22 cp/μl; e Clone I, 51 cp/μl; f Clone L, 78 cp/μl; g Clone U, 102 cp/μl; h.) Clone R, 72 cp/μl; I.) Clones G, P, Z, C, N, and A, 11 cp/μl; j Clones F, T, Y, E, 0 copies detected; and k Clone M, 145 cp/μl. To allow cross-comparison of sample panels, a single threshold for positive amplification was calculated for the entire chip; this value was set to 5 standard deviations above the mean of chambers in the lowest 25% of the intensity range.

Specific Detection of Termite Cluster Treponemes Through Use of a Spirochete-specific

Reverse Primer.

A 16S rRNA gene reverse primer was designed that matched 41 out of 60 termite gut spirochetes with sequence data covering the primer site. Of the known 16S rRNA sequences that did not match the primer, three were associated with the "*termite gut treponeme*" ribotype cluster (26). The remaining mismatches were with sequences affiliated with "*treponeme subgroup I*" (38), which represents less than 1% of spirochetal 16S clones amplified from *Z. nevadensis* using conventional methods and other spirochete-specific primers (*unpublished data*, primers from Lilburn, Schmidt, and Breznak (26)). Our new primers were tested for specificity and efficiency in simplex and multiplex reactions with FTHFS primers/probes using conventional and real-time PCR methods. In on-chip PCR reactions using purified PCR products as template they detected 11% of the expected copy number.

Table 4.1. Sequences Used for Phylogenetic Analysis

Source/Sequence Type	Designation	Gene	Accession	Reference
T. primitia ZAS-1	ZAS-1	16S	AF093251	(22)
T. primitia ZAS-2	ZAS-2	16S	AF093252	(22)
T. azotonutricium ZAS-9	ZAS-9	16S	AF320287	(25)
T. primitia ZAS-1	ZAS-1a	FTHFS	AY162313	(42)
T. primitia ZAS-2	ZAS-2	FTHFS	AY162315	(42)
T. azotonutricium ZAS-9	ZAS-9	FTHFS	AY162316	(42)
Z. angusticollis Gut Clone	A	FTHFS	AY162294	(42)
Z. angusticollis Gut Clone	C	FTHFS	AY162295	(42)
Z. angusticollis Gut Clone	E	FTHFS	AY162296	(42)
Z. angusticollis Gut Clone	E2	FTHFS	AY162297	(42)
Z. angusticollis Gut Clone	F	FTHFS	AY162298	(42)
Z. angusticollis Gut Clone	F2	FTHFS	AY162299	(42)
Z. angusticollis Gut Clone	G	FTHFS	AY162300	(42)
Z. angusticollis Gut Clone	G2	FTHFS	AY162301	(42)
Z. angusticollis Gut Clone	H	FTHFS	AY162302	(42)
Z. angusticollis Gut Clone	I	FTHFS	AY162303	(42)
Z. angusticollis Gut Clone	L	FTHFS	AY162304	(42)
Z. angusticollis Gut Clone	M	FTHFS	AY162305	(42)
Z. angusticollis Gut Clone	N	FTHFS	AY162306	(42)
Z. angusticollis Gut Clone	P	FTHFS	AY162307	(42)
Z. angusticollis Gut Clone	R	FTHFS	AY162308	(42)
Z. angusticollis Gut Clone	T	FTHFS	AY162309	(42)
Z. angusticollis Gut Clone	U	FTHFS	AY162310	(42)
Z. angusticollis Gut Clone	Y	FTHFS	AY162311	(42)
Z. angusticollis Gut Clone	Z	FTHFS	AY162312	(42)
Z. nevadensis Genomovar	ZEG 10.1	FTHFS	DQ420342	This study
Z. nevadensis Genomovar	ZEG 10.2	FTHFS	DQ420343	This study
Z. nevadensis Genomovar	ZEG 10.3	FTHFS	DQ420344	This study
Z. nevadensis Genomovar	ZEG 10.4	FTHFS	DQ420345	This study
Z. nevadensis Genomovar	ZEG 11.1	FTHFS	DQ420346	This study
Z. nevadensis Genomovar	ZEG 11.2	FTHFS	DQ420347	This study
Z. nevadensis Genomovar	ZEG 11.3	FTHFS	DQ420348	This study
Z. nevadensis Genomovar	ZEG 11.4	FTHFS	DQ420349	This study
Z. nevadensis Genomovar	ZEG 11.5	FTHFS	DQ420350	This study
Z. nevadensis Genomovar	ZEG 11.6	FTHFS	DQ420351	This study
Z. nevadensis Genomovar	ZEG 11.7	FTHFS	DQ420352	This study
Z. nevadensis Genomovar	ZEG 12.1	FTHFS	DQ420353	This study
Z. nevadensis Genomovar	ZEG 12.2	FTHFS	DQ420354	This study
Z. nevadensis Genomovar	ZEG 12.3	FTHFS	DQ420355	This study
Z. nevadensis Genomovar	ZEG 12.4	FTHFS	DQ420356	This study
Z. nevadensis Genomovar	ZEG 12.5	FTHFS	DQ420357	This study
Z. nevadensis Genomovar	ZEG 13.1	FTHFS	DQ420358	This study
Z. nevadensis Genomovar	ZEG 10.1	16S	DQ420325	This study
Z. nevadensis Genomovar	ZEG 10.2	16S	DQ420326	This study
Z. nevadensis Genomovar	ZEG 10.3	16S	DQ420327	This study
Z. nevadensis Genomovar	ZEG 10.4	16S	DQ420328	This study
Z. nevadensis Genomovar	ZEG 11.1	16S	DQ420329	This study
Z. nevadensis Genomovar	ZEG 11.2	16S	DQ420330	This study
Z. nevadensis Genomovar	ZEG 11.3	16S	DQ420331	This study
Z. nevadensis Genomovar	ZEG 11.4	16S	DQ420332	This study
Z. nevadensis Genomovar	ZEG 11.5	16S	DQ420333	This study
Z. nevadensis Genomovar	ZEG 11.6	16S	DQ420334	This study

Source/Sequence Type	Designation	Gene	Accession	Reference
Z. nevadensis Genomovar	ZEG 11.7	16S	DQ420335	This study
Z. nevadensis Genomovar	ZEG 12.1	16S	DQ420336	This study
Z. nevadensis Genomovar	ZEG 12.2	16S	DQ420337	This study
Z. nevadensis Genomovar	ZEG 12.3	16S	DQ420338	This study
Z. nevadensis Genomovar	ZEG 12.4	16S	DQ420339	This study
Z. nevadensis Genomovar	ZEG 12.5	16S	DQ420340	This study
Z. nevadensis Genomovar	ZEG 13.1	16S	DQ420341	This study
Z. nevadensis Gut Clone	Zn-FG1	16S	DQ420259	This study
Z. nevadensis Gut Clone	Zn-FG2A	16S	DQ420263	This study
Z. nevadensis Gut Clone	Zn-FG2B	16S	DQ420264	This study
Z. nevadensis Gut Clone	Zn-FG3	16S	DQ420275	This study
Z. nevadensis Gut Clone	Zn-FG4	16S	DQ420273	This study
Z. nevadensis Gut Clone	Zn-FG5A	16S	DQ420269	This study
Z. nevadensis Gut Clone	Zn-FG5C	16S	DQ420270	This study
Z. nevadensis Gut Clone	Zn-FG6	16S	DQ420271	This study
Z. nevadensis Gut Clone	Zn-FG7A	16S	DQ420266	This study
Z. nevadensis Gut Clone	Zn-FG7B	16S	DQ420262	This study
Z. nevadensis Gut Clone	Zn-FG8A	16S	DQ420284	This study
Z. nevadensis Gut Clone	Zn-FG9	16S	DQ420317	This study
Z. nevadensis Gut Clone	Zn-FG10	16S	DQ420319	This study
Z. nevadensis Gut Clone	Zn-FG11A	16S	DQ420272	This study
Z. nevadensis Gut Clone	Zn-FG11B	16S	DQ420258	This study
Z. nevadensis Gut Clone	Zn-FG12	16S	DQ420261	This study
Z. nevadensis Gut Clone	Zn-FG13A	16S	DQ420286	This study
Z. nevadensis Gut Clone	Zn-FG13B	16S	DQ420287	This study
Z. nevadensis Gut Clone	Zn-FG14	16S	DQ420257	This study
Z. nevadensis Gut Clone	Zn-FG15A	16S	DQ420277	This study
Z. nevadensis Gut Clone	Zn-FG15B	16S	DQ420278	This study
Z. nevadensis Gut Clone	Zn-FG15C	16S	DQ420279	This study
Z. nevadensis Gut Clone	Zn-FG16A	16S	DQ420280	This study
Z. nevadensis Gut Clone	Zn-FG16B	16S	DQ420281	This study
Z. nevadensis Gut Clone	Zn-FG17A	16S	DQ420282	This study
Z. nevadensis Gut Clone	Zn-FG17B	16S	DQ420283	This study
Z. nevadensis Gut Clone	Zn-FG18A	16S	DQ420255	This study
Z. nevadensis Gut Clone	Zn-FG18B	16S	DQ420276	This study
Z. nevadensis Gut Clone	Zn-G1	16S	DQ420256	This study
Z. nevadensis Gut Clone	Zn-G2	16S	DQ420254	This study
Z. nevadensis Gut Clone	Zn-G3	16S	DQ420265	This study
Z. nevadensis Gut Clone	Zn-G4A	16S	DQ420310	This study
Z. nevadensis Gut Clone	Zn-G4B	16S	DQ420311	This study
Z. nevadensis Gut Clone	Zn-G4C	16S	DQ420312	This study
Z. nevadensis Gut Clone	Zn-G5A	16S	DQ420313	This study
Z. nevadensis Gut Clone	Zn-G5B	16S	DQ420314	This study
Z. nevadensis Gut Clone	Zn-G6	16S	DQ420260	This study
Z. nevadensis Gut Clone	Zn-G7	16S	DQ420268	This study
Z. nevadensis Gut Clone	Zn-G8	16S	DQ420267	This study
Z. nevadensis Gut Clone	Zn-G9	16S	DQ420315	This study
Z. nevadensis Gut Clone	Zn-G10	16S	DQ420285	This study
Z. nevadensis Gut Clone	Zn-G11	16S	DQ420274	This study
Z. nevadensis Gut Clone	Zn-G12A	16S	DQ420316	This study
Z. nevadensis Gut Clone	Zn-G12B	16S	DQ420324	This study
Z. nevadensis Gut Clone	Zn-G13	16S	DQ420298	This study
Z. nevadensis Gut Clone	Zn-G14	16S	DQ420299	This study
Z. nevadensis Gut Clone	Zn-G15A	16S	DQ420320	This study

Source/Sequence Type	Designation	Gene	Accession	Reference
Z. nevadensis Gut Clone	Zn-G15B	16S	DQ420321	This study
Z. nevadensis Gut Clone	Zn-G15C	16S	DQ420322	This study
Z. nevadensis Gut Clone	Zn-G16	16S	DQ420300	This study
Z. nevadensis Gut Clone	Zn-G17	16S	DQ420301	This study
Z. nevadensis Gut Clone	Zn-G18	16S	DQ420302	This study
Z. nevadensis Gut Clone	Zn-G19	16S	DQ420303	This study
Z. nevadensis Gut Clone	Zn-G20	16S	DQ420323	This study
Z. nevadensis Gut Clone	Zn-FS1	16S	DQ420288	This study
Z. nevadensis Gut Clone	Zn-FS2	16S	DQ420289	This study
Z. nevadensis Gut Clone	Zn-S1A	16S	DQ420307	This study
Z. nevadensis Gut Clone	Zn-S2	16S	DQ420295	This study
Z. nevadensis Gut Clone	Zn-S3	16S	DQ420308	This study
Z. nevadensis Gut Clone	Zn-S4A	16S	DQ420309	This study
Z. nevadensis Gut Clone	Zn-S5	16S	DQ420296	This study
Z. nevadensis Gut Clone	Zn-S6	16S	DQ420297	This study
Z. nevadensis Gut Clone	Zn-S7A	16S	DQ420304	This study
Z. nevadensis Gut Clone	Zn-S7B	16S	DQ420305	This study
Z. nevadensis Gut Clone	Zn-S8	16S	DQ420290	This study
Z. nevadensis Gut Clone	Zn-S9	16S	DQ420291	This study
Z. nevadensis Gut Clone	Zn-S10	16S	DQ420292	This study
Z. nevadensis Gut Clone	Zn-S11A	16S	DQ420306	This study
Z. nevadensis Gut Clone	Zn-S12	16S	DQ420293	This study
Z. nevadensis Gut Clone	Zn-S13	16S	DQ420294	This study
Acetonema longum	APO-1	16S	M61919	(19)
Acholeplasma laidlawii	JA1	16S	M23932	(54)
Clostridium mayombei	SFC-5	16S	M62421	(18)
Comamonadaceae Clone	C-6	16S	AF523013	(29)
N. koshunensis symbiont	Nk-S93	16S	AB084970	(34)
R. flavipes Gut Clone	RFS88	16S	AF068344	(26)
R. santonensis Gut Clone	RsaHf236	16S	AY571482	(58)
R. santonensis Gut Clone	RsaHf303	16S	AY571478	(58)
R. speratus Gut Clone	Rs-B05	16S	AB088896	(15)
R. speratus Gut Clone	Rs-B10	16S	AB088880	(15)
R. speratus Gut Clone	Rs-B29	16S	AB088891	(15)
R. speratus Gut Clone	Rs-D17	16S	AB089048	(15)
R. speratus Gut Clone	Rs-D39	16S	AB089089	(15)
R. speratus Gut Clone	Rs-D40	16S	AB088874	(15)
R. speratus Gut Clone	Rs-D46	16S	AB088865	(15)
R. speratus Gut Clone	Rs-E47	16S	AB088921	(15)
R. speratus Gut Clone	Rs-F14	16S	AB088939	(15)
R. speratus Gut Clone	Rs-F63	16S	AB088934	(15)
R. speratus Gut Clone	Rs-E64	16S	AB088888	(15)
R. speratus Gut Clone	Rs-K70	16S	AB089106	(15)
R. speratus Gut Clone	Rs-M74	16S	AB089115	(15)
R. speratus Gut Clone	Rs-P59	16S	AB088914	(15)
R. speratus Gut Clone	Rs-Q39	16S	AB089075	(15)
Sporomusa termitida	JSN-2	16S	M61920	(19)
Termitobacter aceticus	SYR	16S	Z49863	(13)
TM7 phylum Env. Clone	BU080	16S	AF385568	
Treponema amylovorum	HA2P	16S	Y09959	(56)
Treponema denticola	II:11:33520	16S	M71236	(38)
Treponema maltophilum	patient BR	16S	X87140	(57)
Treponema pallidum	Nichols	16S	M88726	(38)
Treponema phagedenis	K5	16S	M57739	(38)

References

1.   Assuming a Poisson distribution, if 67% percent of chambers are empty then the expected number of cells per chamber is -ln 0.67 or 0.40. The probability that a chamber contains more than one cell is 1 - 0.67 – ((e^-0.40)*(0.40^1))/(1!) or 6.2%

2.   Value ± one standard deviation, 13 termites served as source of cells for n=32 sample panels. All sample panels that met our conditions for single cell separation and contained at least one FTHFS-positive chamber were used in calculation of gut bacterial loads.

3.   The binomial distribution function was used to calculate the probability that, in 13 out of 28 trials, a sequence that is present in 5 percent (0 out of 20 16S-only chambers) of chambers would randomly co-localize with Clone H Group FTHFS sequences.

4.   **Acinas, S. G., R. Sarma-Rupavtarm, V. Klepac-Ceraj, and M. F. Polz.** 2005. PCR-induced sequence artifacts and bias: Insights from comparison of two 16S rRNA clone libraries constructed from the same sample. Appl Environ Microbiol **71:**8966-8969.

5.   **Amann, R. I., W. Ludwig, and K. H. Schleifer.** 1995. Phylogenetic identification and *in situ* detection of individual microbial cells without cultivation. Microbiol Rev **59:**143-169.

6.   **Ashelford, K. E., N. A. Chuzhanova, J. C. Fry, A. J. Jones, and A. J. Weightman.** 2005. At least 1 in 20 16S rRNA sequence records currently held in

public repositories is estimated to contain substantial anomalies. Appl Environ Microbiol **71:**7724-7736.

7. **Béjà, O., L. Aravind, E. V. Koonin, M. T. Suzuki, A. Hadd, L. P. Nguyen, S. B. Jovanovich, C. M. Gates, R. A. Feldman, J. L. Spudich, E. N. Spudich, and E. F. DeLong.** 2000. Bacterial rhodopsin: evidence for a new type of phototrophy in the sea. Science **289:**1902-1906.

8. **Brauman, A., M. D. Kane, M. Labat, and J. A. Breznak.** 1992. Genesis of acetate and methane by gut bacteria of nutritionally diverse termites. Science **257:**1384-1387.

9. **Breznak, J. A., and H. S. Pankratz.** 1977. In situ morphology of the gut microbiota of wood-eating termites [*Reticulitermes flavipes* (Kollar) and *Coptotermes formosanus* Shiraki]. Appl Environ Microbiol **33:**406-426.

10. **Breznak, J. A., and J. M. Switzer.** 1986. Acetate synthesis from H_2 plus CO_2 by termite gut microbes. Appl Environ Microbiol **52:**623-630.

11. **Corless, C. E., M. Guiver, R. Borrow, V. Edwards-Jones, E. B. Kaczmarski, and A. J. Fox.** 2000. Contamination and sensitivity issues with a real-time universal 16S rRNA PCR. J Clin Microbiol **38:**1747-1752.

12. **Gray, N. D., and I. M. Head.** 2001. Linking genetic identity and function in communities of uncultured bacteria. Environ Microbiol **3:**481-492.

13. **GrechMora, I., M. L. Fardeau, B. K. C. Patel, B. Ollivier, A. Rimbault, G. Prensier, J. L. Garcia, and E. GarnierSillam.** 1996. Isolation and characterization of *Sporobacter termitidis* gen nov sp nov, from the digestive tract

of the wood-feeding termite *Nasutitermes lujae*. Int J Syst Evol Microbiol **46:**512-518.

14. **Hong, J. W., and S. R. Quake.** 2003. Integrated nanoliter systems. Nat Biotechnol **21:**1179-1183.

15. **Hongoh, Y., M. Ohkuma, and T. Kudo.** 2003. Molecular analysis of bacterial microbiota in the gut of the termite *Reticulitermes speratus* (Isoptera; Rhinotermitidae). FEMS Microbiol Ecol **44:**231-242.

16. **Huber, T., G. Faulkner, and P. Hugenholtz.** 2004. Bellerophon: a program to detect chimeric sequences in multiple sequence alignments. Bioinformatics **20:**2317-2319.

17. **Hugenholtz, P., B. M. Goebel, and N. R. Pace.** 1998. Impact of culture-independent studies on the emerging phylogenetic view of bacterial diversity. J Bacteriol **180:**4765-4774.

18. **Kane, M. D., A. Brauman, and J. A. Breznak.** 1991. *Clostridium mayombei* sp. nov., an H2/CO2 acetogenic bacterium from the gut of the African soil-feeding termite, *Cubitermes speciosus*. Arch Microbiol **156:**99-104.

19. **Kane, M. D., and J. A. Breznak.** 1991. *Acetonema longum* gen. nov. sp. nov., an H2/CO2 acetogenic bacterium from the termite, *Pterotermes occidentis*. Arch Microbiol **156:**91-98.

20. **Lane, D. J.** 1991. 16S/23S rRNA sequencing, p. 115-175. *In* M. G. E. Stackebrandt (ed.), Nucleic Acid Techniques in Bacterial Systematics. Wiley, New York.

21. **Leadbetter, J. R., and J. A. Breznak.** 1996. Physiological ecology of *Methanobrevibacter cuticularis* sp. nov. and *Methanobrevibacter curvatus* sp. nov., isolated from the hindgut of the termite *Reticulitermes flavipes*. Appl Environ Microbiol **62:**3620-3631.

22. **Leadbetter, J. R., T. M. Schmidt, J. R. Graber, and J. A. Breznak.** 1999. Acetogenesis from H_2 plus CO_2 by spirochetes from termite guts. Science **283:**686-689.

23. **Leaphart, A. B., M. J. Friez, and C. R. Lovell.** 2003. Formyltetrahydrofolate synthetase sequences from salt marsh plant roots reveal a diversity of acetogenic bacteria and other bacterial functional groups. Appl Environ Microbiol **69:**693-696.

24. **Leaphart, A. B., and C. R. Lovell.** 2001. Recovery and analysis of formyltetrahydrofolate synthetase gene sequences from natural populations of acetogenic bacteria. Appl Environ Microbiol **67:**1392-1395.

25. **Lilburn, T. G., K. S. Kim, N. E. Ostrom, K. R. Byzek, J. R. Leadbetter, and J. A. Breznak.** 2001. Nitrogen fixation by symbiotic and free-living spirochetes. Science **292:**2495-2498.

26. **Lilburn, T. G., T. M. Schmidt, and J. A. Breznak.** 1999. Phylogenetic diversity of termite gut spirochaetes. Environ Microbiol **1:**331-345.

27. **Ljungdahl, L. G.** 1986. The autotrophic pathway of acetate synthesis in acetogenic bacteria. Ann Rev Microbiol **40:**415-450.

28. **Lovell, C. R., and A. B. Leaphart.** 2005. Community-level analysis: key genes of CO2-reductive acetogenesis. Methods Enzymol **397:**454-469.

29.   **Loy, A., W. Beisker, and H. Meier.** 2005. Diversity of bacteria growing in natural mineral water after bottling. Appl Environ Microbiol **71:**3624-3632.

30.   **Ludwig, W., O. Strunk, R. Westram, L. Richter, H. Meier, Yadhukumar, A. Buchner, T. Lai, S. Steppi, G. Jobb, W. Förster, I. Brettske, S. Gerber, A. W. Ginhart, O. Gross, S. Grumann, S. Hermann, R. Jost, A. König, T. Liss, R. Lüßmann, M. May, B. Nonhoff, B. Reichel, R. Strehlow, A. Stamatakis, N. Stuckmann, A. Vilbig, M. Lenke, T. Ludwig, A. Bode, and K. H. Schleifer.** 2004. ARB: a software environment for sequence data. Nucl Acids Res **32:**1363-1371.

31.   **Manefield, M., A. S. Whiteley, R. I. Griffiths, and M. J. Bailey.** 2002. RNA stable isotope probing, a novel means of linking microbial community function to phylogeny. Appl Environ Microbiol **68:**5367-5373.

32.   **Nadkarni, M. A., F. E. Martin, N. A. Jacques, and N. Hunter.** 2002. Determination of bacterial load by real-time PCR using a broad-range (universal) probe and primers set. Microbiol **148:**257-266.

33.   **Nielsen, J. L., D. Christensen, M. Kloppenborg, and P. H. Nielsen.** 2003. Quantification of cell-specific substrate uptake by probe-defined bacteria under *in situ* conditions by microautoradiography and fluorescence *in situ* hybridization. Environ Microbiol **5:**202-211.

34.   **Noda, S., M. Ohkuma, A. Yamada, Y. Hongoh, and T. Kudo.** 2003. Phylogenetic position and in situ identification of ectosymbiotic spirochetes on protists in the termite gut. Appl Environ Microbiol **69:**625-633.

35.   **Odelson, D. A., and J. A. Breznak.** 1983. Volatile fatty acid production by the hindgut microbiota of xylophagous termites. Appl Environ Microbiol **45:**1602-1613.

36.   **Ohkuma, M., and T. Kudo.** 1996. Phylogenetic diversity of the intestinal bacterial community in the termite *Reticulitermes speratus*. Appl Environ Microbiol **62:**461-468.

37.   **Pang, H., and H. H. Winkler.** 1993. Copy number of the 16S rRNA gene in *Rickettsia prowazekii*. J Bacteriol **175:**3893-3896.

38.   **Paster, B. J., F. E. Dewhirst, W. G. Weisburg, L. A. Tordoff, G. J. Fraser, R. B. Hespell, T. B. Stanton, L. Zablen, L. Mandelco, and C. R. Woese.** 1991. Phylogenetic analysis of the spirochetes. J Bacteriol **173:**6101-6109.

39.   **Pester, M., and A. Brune.** 2006. Expression profiles of fhs (FTHFS) genes support the hypothesis that spirochaetes dominate reductive acetogenesis in the hindgut of lower termites. Environ Microbiol **8:**1261-1270.

40.   **Rainey, F. A., N. L. Ward-Rainey, P. H. Janssen, H. Hippe, and E. Stackebrandt.** 1996. *Clostridium paradoxum* DSM 7308T contains multiple 16S rRNA genes with heterogeneous intervening sequences. Microbiol **142:**2087-2095.

41.   **Riesenfeld, C. S., P. D. Schloss, and J. Handelsman.** 2004. Metagenomics: Genomic analysis of microbial communities. Ann Rev Genet **38:**525-552.

42.   **Salmassi, T. M., and J. R. Leadbetter.** 2003. Analysis of genes of tetrahydrofolate-dependent metabolism from cultivated spirochaetes and the gut community of the termite *Zootermopsis angusticollis*. Microbiol **149:**2529-2537.

43. **Schmidt, H. A., K. Strimmer, M. Vingron, and A. von Haeseler.** 2002. TREE-PUZZLE: maximum likelihood phylogenetic analysis using quartets and parallel computing. Bioinformatics **18:**502-504.

44. **Sogin, S. J., M. L. Sogin, and C. R. Woese.** 1971. Phylogenetic measurement in procaryotes by primary structural characterization. J Mol Evol **1:**173-184.

45. **Strous, M., E. Pelletier, S. Mangenot, T. Rattei, A. Lehner, M. W. Taylor, M. Horn, H. Daims, D. Bartol-Mavel, P. Wincker, V. Barbe, N. Fonknechten, D. Vallenet, B. Segurens, C. Schenowitz-Truong, C. Médigue, A. Collingro, B. Snel, B. E. Dutilh, H. J. Op den Camp, C. van der Drift, I. Cirpus, K. T. van de Pas-Schoonen, H. R. Harhangi, L. van Niftrik, M. Schmid, J. Keltjens, J. van de Vossenberg, B. Kartal, H. Meier, D. Frishman, M. A. Huynen, H. W. Mewes, J. Weissenbach, M. S. Jetten, M. Wagner, and D. Le Paslier.** 2006. Deciphering the evolution and metabolism of an anammox bacterium from a community genome. Nature **440:**790-794.

46. **Suzuki, M. T., L. T. Taylor, and E. F. DeLong.** 2000. Quantitative analysis of small-subunit rRNA genes in mixed microbial populations via 5'-nuclease assays. Appl Environ Microbiol **66:**4605-4014.

47. **Tholen, A., and A. Brune.** 2000. Impact of oxygen on metabolic fluxes and *in situ* rates of reductive acetogenesis in the hindgut of the wood-feeding termite *Reticulitermes flavipes*. Environ Microbiol **2:**436-449.

48. **Thorsen, T., S. J. Maerkl, and S. R. Quake.** 2002. Microfluidic large-scale integration. Science **298:**580-584.

49.   **Tringe, S. G., C. von Mering, A. Kobayashi, A. A. Salamov, K. Chen, H. W. Chang, M. Podar, J. M. Short, E. J. Mathur, J. C. Detter, P. Bork, P. Hugenholtz, and E. M. Rubin.** 2005. Comparative metagenomics of microbial communities. Science **308:**554-557.

50.   **Tyson, G. W., J. Chapman, P. Hugenholtz, E. E. Allen, R. J. Ram, P. M. Richardson, V. V. Solovyev, E. M. Rubin, D. S. Rokhsar, and J. F. Banfield.** 2004. Community structure and metabolism through reconstruction of microbial genomes from the environment. Nature **428:**37-43.

51.   **Venter, J. C., K. Remington, J. F. Heidelberg, A. L. Halpern, D. Rusch, J. A. Eisen, D. Wu, I. Paulsen, K. E. Nelson, W. Nelson, D. E. Fouts, S. Levy, A. H. Knap, M. W. Lomas, K. Nealson, O. White, J. Peterson, J. Hoffman, R. Parsons, H. Baden-Tillson, C. Pfannkoch, Y. H. Rogers, and H. O. Smith.** 2004. Environmental genome shotgun sequencing of the Sargasso Sea. Science **304:**66-74.

52.   **Vogelstein, B., and K. W. Kinzler.** 1999. Digital PCR. Proc Natl Acad Sci USA **96:**9236-9241.

53.   **Warren, L., D. Bryder, I. L. Weissman, and S. R. Quake.** 2006. Transcription factor profiling in individual hematopoietic progenitors by digital RT-PCR. Proc Natl Acad Sci USA **103:**17807-17812.

54.   **Weisburg, W. G., J. G. Tully, D. L. Rose, J. P. Petzel, H. Oyaizu, D. Yang, L. Mandelco, J. Sechrest, T. G. Lawrence, J. Van Etten, and et al.** 1989. A phylogenetic analysis of the mycoplasmas: basis for their classification. J Bacteriol **171:**6455-6467.

55. **Winston, P. W., Bates, Donald H.** 1960. Saturated solutions for the control of humidity in biological research. Ecology **41:**232-237.

56. **Wyss, C., B. K. Choi, P. Schüpbach, B. Guggenheim, and U. B. Göbel.** 1997. *Treponema amylovorum* sp. nov., a saccharolytic spirochete of medium size isolated from an advanced human periodontal lesion. Int J Syst Bacteriol **47:**842-845.

57. **Wyss, C., B. K. Choi, P. Schüpbach, B. Guggenheim, and U. B. Göbel.** 1996. *Treponema maltophilum* sp. nov., a small oral spirochete isolated from human periodontal lesions. Int J Syst Bacteriol **46:**745-752.

58. **Yang, H., D. Schmitt-Wagner, U. Stingl, and A. Brune.** 2005. Niche heterogeneity determines bacterial community structure in the termite gut (*Reticulitermes santonensis*). Environ Microbiol **7:**916-932.

59. **Zhang, K., A. C. Martiny, N. B. Reppas, K. W. Barry, J. Malek, S. W. Chisholm, and G. M. Church.** 2006. Sequencing genomes from single cells by polymerase cloning. Nat Biotechnol **24:**680-686.

60. **Zuckerkandl, E., and L. Pauling.** 1965. Molecules as documents of evolutionary history. J Theor Biol **8:**357-366.

61. **Zwirglmaier, K., W. Ludwig, and K. H. Schleifer.** 2004. Recognition of individual genes in a single bacterial cell by fluorescence *in situ* hybridization - RING-FISH. Mol Microbiol **51:**89-96.